*Desalination and Water Treatment*
www.deswater.com

doi: 10.5004/dwt.2022.28359

256 (2022) 221–234
April

# Understanding the role of the radiometric indices in temporal evapotranspiration estimation in arid environments

Sajjad Hussain[a], Jarbou Bahrawi[a], Muhammad Awais[b], Mohamed Elhag[d,e,f,g,*]

[a]*Department of Hydrology and Water Resources Management, Faculty of Meteorology, Environment & Arid Land Agriculture, King Abdulaziz University, Jeddah 21589, Saudi Arabia, emails: melhag@kau.edu.sa (M. Elhag), smuhammadsingle@stu.kau.edu.sa (S. Hussain), jbahrawi@kau.edu.sa (J. Bahrawi)*
[b]*Research Center of Fluid Machinery Engineering and Technology, Jiangsu University, Zhenjiang 212013, China, email: awais@ujs.edu.cn*
[c]*Department of Applied Geosciences, Faculty of Science, German University of Technology in Oman, Muscat 1816, Oman*
[d]*Department of Hydrology and Water Resources Management, Faculty of Meteorology, Environment and Arid Land Agriculture, King Abdulaziz University, Jeddah 21589, Saudi Arabia, email: melhag@kau.edu.sa*
[e]*Institute of Remote Sensing and Digital Earth (RADI), Chinese Academy of Science (CAS), Beijing 100094, China*
[f]*Department of Applied Geosciences, Faculty of Science, German University of Technology in Oman, Muscat 1816, Oman*
[g]*Department of Geoinformation in Environmental Management, CI-HEAM/Mediterranean Agronomic Institute of Chania, Chania 73100, Greece*

Received 20 September 2021; Accepted 4 March 2022

**ABSTRACT**

In water budget assessment, evapotranspiration (ET) proved as one of the most significant features whose reputation boosts in arid climates. Indirect approaches to estimate ET are complex in their calculation requiring different algorithms but an indirect approach was taken in this study which enables us to develop relationships, which are less complex and less time-consuming. In this study, an association between ET, observed by the Global Land Data Assimilation System of National Aeronautics and Space Administration and vegetation indices (VI) taken by Landsat 8 images were generated. Quarterly images were taken for the period of two years (2018–2019) to make an empirical relationship by linear regression analysis between ET and VI's specifically named as, soil adjusted vegetation index (SAVI), normalized difference vegetation index (NDVI), and normalized difference water index (NDWI). The resultant equation represents the relationship in terms of $R^2$ enabling to evaluate each index with ET. NDVI was found averagely associated with ET estimation because of its low regression value, in general, it goes minimum up to 0.56 for August 2019. However, it remains approximately consistent between 0.60 and 0.65 for all month except October 18 in which its values go to 0.72. Similarly, SAVI was also analyzed and got much better correlation for both years sustaining near or above 0.65 with a maximum value of 0.78, so this index performed well then NDVI. Likewise, to other indices, NDWI was also studied and got very splendid results of correlation than other two indices. This index sustains its values of $R^2$ among 0.85–0.91 for maximum months of the years indicating its highest relationship with ET. It can be concluded that NDWI derived relations were more promising than the other two for ET calculation.

*Keywords:* Evapotranspiration; Vegetation indices; Normalized difference vegetation index; Normalized difference water index; Soil adjusted vegetation index; Global Land Data Assimilation System

* Corresponding author.

*Presented at the 8th International Conference on Sustainable Solid Waste Management (Thessaloniki 2021), 23–25 June 2021, Virtual Conference*

## 1. Introduction

Evapotranspiration (ET), which involves the process of moisture transfer from the earth-cum-plants to the biosphere throughout the day and night, is one of the fundamental processes in integrated water management. ET is caused by a differential in vapor pressure between the non-boring atmosphere and the evaporating surface. The phenomenon of ET also considered a fundamental part of consumptive use estimation in the field of agriculture. In the same manner, estimation of ET directly relates to water use efficiency, enhancing its importance in water resources [1]. The introduction of ET into the hydrologic cycle is influenced by local weather variables such as radiation, ambient temperature, soil moisture, wind speed, rainfall, and humidity [2]. Techniques to estimate ET mainly of field scale including, pan evaporation, Penman–Monteith, eddy covariance (EC), and lysimeter systems [3]. These field procedures have different constraints like expensiveness to setup especially in underdeveloped areas, also in those areas where the weather condition is severe. Other than these direct estimations indirect techniques are there which involve empirical approach of ET calculation by providing the ability to overcome the limitation which came in the direct ET estimation and also such type of work does not require global scale parameters. Empirical approaches are primarily based on the notion of energy balance, which may be broken down into three basic components: temperature, solar radiation, and empirical approach equations. Although, these techniques have the accuracy of estimation but such methods are not capable of providing data with capability of fine spatial and temporal resolution, specifically where climate is harsh [4]. Remote sensing (RS) techniques have been proven to be very promising as a result of these factors, particularly because studies have introduced a wide range of wave bandwidths [5–7]. Satellite-based remote sensing provides high special and temporal resolution, so their use in estimation of ET enhances data measurement accuracy for other hydrological processes. Similarly, the Global Land Data Assimilation System (GLDAS) was established to obtain better accuracy in findings by combining ground and satellite observation. This setup combines a model of the land surface as well as ground simulation procedures to offer flux of the land surface and their states [8]. GLDAS provide data with spatial resolution of 0.25° and temporal resolution of 3 h to overcome various limitation in direct ET measuring practices. The assimilation data have already been used for water shortage studies by many researchers [9,10]. Validation of evapotranspiration of GLDAS was practiced by Hongwei for the river basin of Heihe in which he integrates Taylor equation with Ts-NDVI [11–13].

Vegetation indices (VI), which are based on green plant density, are another method of forecasting ET [14]. These indices employ visible and infrared bands with wavelengths ranging from 850 to 850 nm, which are commonly found on satellite products [15]. Numerous investigations were conducted to examine the relationship between VI and ground parameters such as ET and crop coefficient (Kc) from ground level to big scale satellite [16,17]. The main objective of VI relation is to enforce the argument that ET can be measured by alternative technique of VI as per indicated in preceding researches. Normalized difference vegetation index (NDVI) act as vegetation indicator which can be measured by numerous techniques of remote-sensing providing traces to approximate ET. NDVI has a strong linkage to calculate different parameters, like fractional vegetation cover which helps in finding ET for mixed landscape [18,19]. Higher values of NDVI indicate higher stomatal activity which indirectly indicates the higher level of vegetation, while by longer study it can estimate the crop yield and drought assessment [20,21]. It also used to derive crop coefficients for different agricultural fields which helps to determine water stress conditions [22,23]. The empirical relationship between NDVI and reference evapotranspiration was constructed and validated, yielding strong linear regression coefficients [24]. Satellites from which direct ET has been computed is off larger pixel extent which covers large spatial area, so instead of this, Landsat 8 satellite provides resolution of 30 m × 30 m with near-infrared (NIR) and red band providing high spatial resolution value of NDVI [25]. So, the relation among courser and high pixel products could lead to a better result in water management. Normalized difference water index (NDWI) have strong relativeness to plant water content which leads to estimate plant water stress [6,26]. According to Jovanovic et al. [25], who researched the relationship between NDWI and ET using several remote sensing techniques and validating them with ground measurements in 2014, the co-relation coefficient can reach 0.90, suggesting their substantial relativeness [27]. Soil adjusted vegetation index (SAVI) had been developed to reduce the impact of soil brightness. Generally, a correction factor of 0.5 has been considered for normal environmental conditions, while it may vary on provisional basis. In a comparative study of VI in the Kuwait region 0.9 value was proposed [28]. Caturegli et al. [24] analyzed $ET_{ref}$ relations with several VI in 2019 and discovered a very promising correlation, from which SAVI performed considerably better and gave $R^2$ of 0.90. Likewise, Chowdhury and Al-Zahrani [29] also researched the linkage between ET and different VI's for the area of Southwestern USA and resulted in a high correlation among each other and similar researches can be seen in these articles.

The major goal of this study is to look at the relationship between three main indices (NDVI, NDWI, and SAVI) obtained from Landsat 8 and the GLDAS based ET model. The novelty of this study is to seeks understanding of seasonal behavior of the ET-VI relationship in arid climates and to determine which index perform well in temperate climates. This study will also encourage the use of relational estimation of ET rather than sophisticated energy balance calculations [42]. For further research, various combinations of indices can be used to find strong relativeness with ET.

## 2. Material and methods

### 2.1. Study area description

Saudi Arabia (24°N, 45°E) is largest state situated of western Asia. This country has 2.15 million km$^2$ with very minor (112 mm/y) amount of precipitation [30]. Cereals, vegetables, and fodder crops, primarily alfalfa, make up the majority of kingdoms crops.

Saudi Arabia's water demand is extremely competitive, with agricultural accounting for 83%–90% of total demand [31]. Therefore, non-precise application of water could lead to water unbalance among different sectors, for that (ET) can play a vital role [30]. The selected area is located in north-western part of Saudi Arabia between 29°–32° N to 36°–40° E and one of the highly agricultural province named Al-Jawf [32]. Most of the area has been cultivated under center pivot irrigation system by commercial growers (Fig. 1). Developed techniques such as center pivot have increased the agricultural area in this region from zero to 1,500 km$^2$ in a few years, primarily irrigated by groundwater, and the province has cultivated more than 0.8 million ha of alfalfa, accounting for 54% of total alfalfa cultivated in Saudi Arabia [33].

### 2.2. Methodology

The main data sets were acquired from Landsat 8 OLI satellite and GLDAS. Geological Information System (GIS) based ArcMap 10.6 software was used to process all images and perform raster calculations.

Pre-processing included importing appropriate file formats, sub-setting band layers, and re-projecting all of the imagery. Then, using the techniques outlined in section 2.3.2, vegetation indices (NDVI, SAVI, and NDWI) were generated. Sample values were then extracted for statistical analysis and estimation of agreement between both variables (Fig. 2 representing general methodology).

### 2.3. Data description and collection

#### 2.3.1. Global Land Data Assimilation System

This system is a joint collaboration between the National Aeronautics and Space Administration (NASA), National Oceanic and Atmospheric Administration (NOAA), National Centers for Environmental Prediction (NCEP). GLDAS provides global data with a wide range of variables at high resolution by combining satellite and ground observation data with a land surface model and data assimilation approach. The above technique been used in simulation of water flux and energy balance among the atmosphere and land surface [8]. Datasets for this study were obtained from the Goddard Earth Sciences Data and Information Services Centre (GES DISC) website, which provide GLDAS NOAH 025 3H v2.1 evapotranspiration at spatial resolution of 0.25° with 3 h interval in GeoTIFF format on which the VI's was calculated (website: https://giovanni.gsfc.nasa.gov, accessed on October-2020). After obtaining the data then converted to mm/d for batter comparison. Because of insufficient monitoring of ET, it's estimation at a regional scale is problematic. In this case, satellite-based remote sensing is typically utilized to calculate energy balance based on surface temperature measurements [34–36]. In this approach, a satellite called Gravity Recovery and Climate Experiment (GRACE) was used to estimate water storage with a difference of 30-d observation and implemented to drainage basin water balance equation as given:

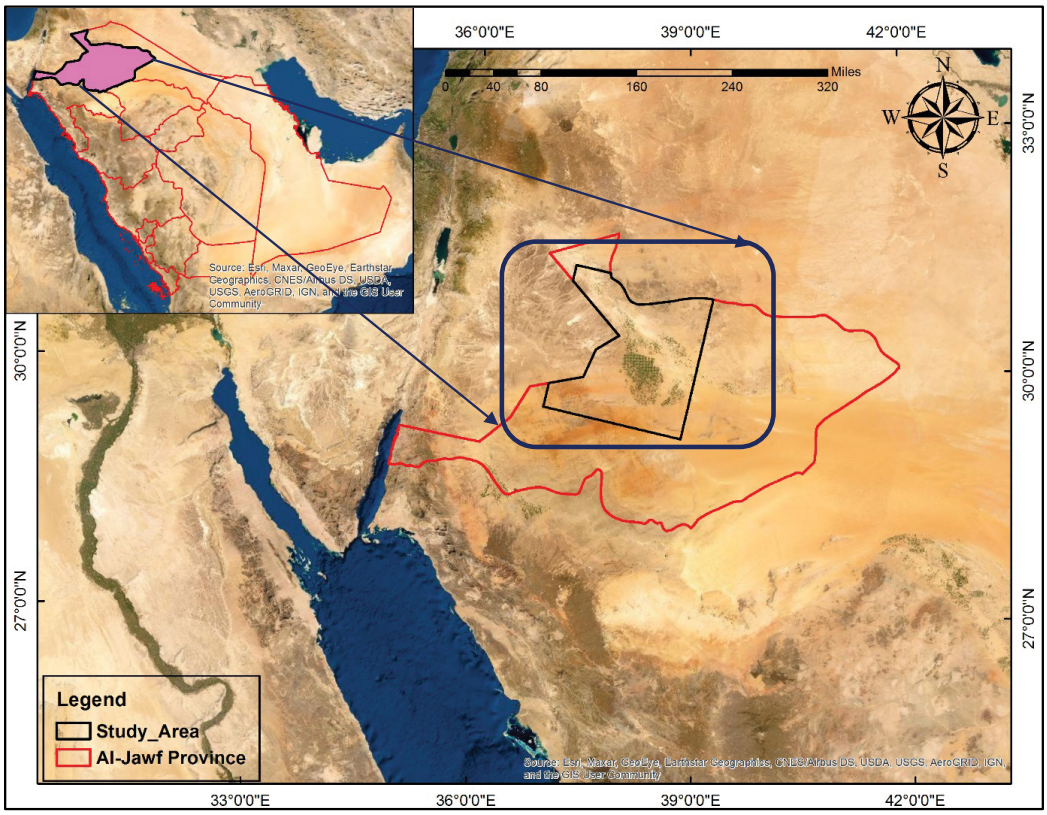


Fig. 1. Study area in Al-Jawf Province, Saudi Arabia.

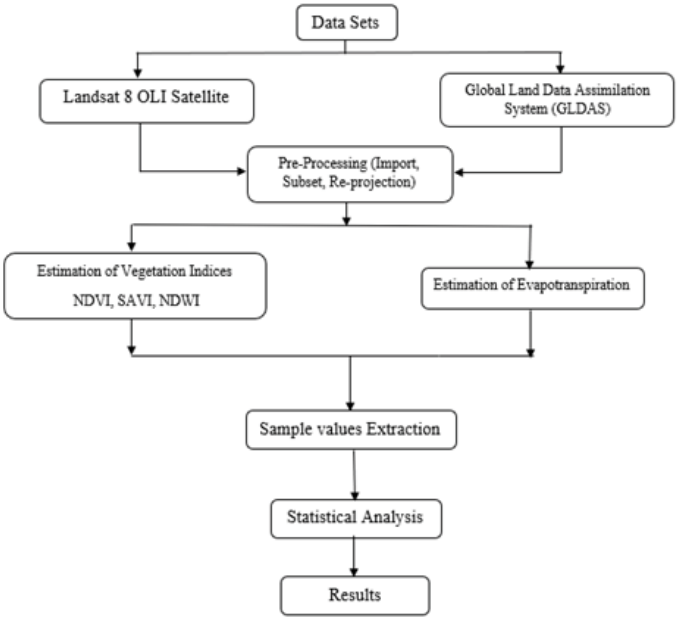


Fig. 2. Methodology flowchart.

$$S_{2,1} - S_{1,1} = \sum_{1,1}^{2,1} P - \sum_{1,1}^{2,1} \mathrm{ET} - \sum_{1,1}^{2,1} Q \tag{1}$$

Storage is represented by $S$, precipitation by P, evapotranspiration by ET, and basin discharge by $Q$, which is the integral of the observation time. As a result of the simplification, the equation may be written as:

$$\Delta S = \frac{1}{N} \sum_{n=1}^{N} \sum_{d=D1+n}^{D2+n-1} \left(P_d - \mathrm{ET}_d - Q_d\right) \tag{2}$$

where $\Delta S$ indicates variation in water storage on average basis, $N$ is number of observing days, $D$,$d$ represents first and observation day respectively. Owing to non-consecutive and varying length of GRACE Eq. (2) would be expanded as:

$$\Delta S = \sum_{d=D}^{D+N-1} \frac{d-D}{N} \left(P_d - \mathrm{ET}_d - Q_d\right) + \sum_{d=D+N}^{D-1} \left(P_d - \mathrm{ET}_d - Q_d\right) + \sum_{d=D}^{D+N-1} \left(P_d - \mathrm{ET}_d - Q_d\right) \frac{D+N-d}{N} \tag{3}$$

In order to attain ET, Eq. (3) must be divided by effective observation days $N$ [Eq. (4)]. As, $\Delta S$ approximate the variation in storage by GRACE satellite but normally it's not used in hydrology, due to this model was made for identical GRACE periods by equating the right side of Eq. (5) divided by $N$, with the $P$ and $Q$ terms set to zero.

$$N = \left\{ \frac{\left(N_1 - 1\right)}{2} + \left[ D_2 - \left(D_2 + N_1\right) \right] + \frac{\left(N_2 - 1\right)}{2} \right\} \tag{4}$$

$$V_{\mathrm{ET}} = \frac{1}{p - Q - \Delta s} \sqrt{V_p^2 p^2 + V_Q^2 Q^2 + V_{\Delta S}^2 \Delta S^2} \tag{5}$$

where $V_{\mathrm{ET}}$ indicates the relative error with 95% confidence interval, $V_{\Delta S} \Delta S$ represents absolute error of monthly water storage by GRACE. It also comprises of errors coming from GRACE instrument and signal retrieval, atmospheric mass variation and leakage.

### 2.3.2. NDVI, SAVI & NDWI by Landsat 8

The remote sensing images of Landsat 8 were acquired from United States Geological Survey (USGS) website for 2018–2019 (website: https://earthexplorer.usgs.gov, accessed on October-2020). It was priorities to select no cloud images for study to avoid image corrections. The images taken by the satellite (Landsat 8) have fine spatial resolution of 30 m × 30 m with temporal resolution of 8 d. All images were acquired with row 37 and path 172 with WGS-1984 projection system. Furthermore, time of acquisition, cloud cover, sun elevation is presented in Table 1.

NDVI is a widely used for water resource and hydrologic applications, with values range between +1 to –1, indicating area covered by vegetation and non-vegetative proportion respectively. Some of the negative values can be observed for NDVI which might indicate water bodies, cloud cover, complete desert, or snow [37]. Spectral response of soil with barren lands and rocks normally approaches to zero [38,39]. This index can be calculated by the reflectance of the near-infrared and red band using the following equation:

$$\mathrm{NDVI} = \frac{\rho\mathrm{NIR} - \rho\mathrm{Red}}{\rho\mathrm{NIR} + \rho\mathrm{Red}} \tag{6}$$

Likewise, to NDVI, another index namely SAVI was used in the research which decreases reflectance of soil influence on vegetation. This index enables the researchers to develop a global model for the dynamic soil-vegetation system and can be calculated by using the formula [35]:

Table 1
Satellite image parameters

| Image number | Parameters | | | |
|---|---|---|---|---|
| | Satellite | Date | Sun elevation (°) | Time (GMT) |
| 1st | | 09-01-18 | 33.99 | 7:59 |
| 2nd | | 14-03-18 | 50.64 | 7:58 |
| 3rd | | 04-07-18 | 67.90 | 7:58 |
| 4th | | 08-10-18 | 48.40 | 8:05 |
| 5th | Landsat 8 | 11-12-18 | 34.44 | 7:59 |
| 6th | | 18-04-19 | 62.33 | 7:59 |
| 7th | | 07-07-19 | 67.79 | 7:59 |
| 8th | | 09-09-19 | 58.82 | 8:00 |
| 9th | | 30-12-19 | 33.57 | 7:53 |

$$\mathrm{SAVI} = \frac{\rho\mathrm{NIR} - \rho\mathrm{Red}}{\rho\mathrm{NIR} + \rho\mathrm{Red} + L}\left(1 + L\right) \tag{7}$$

where ρ is spectral reflectance of Landsat image band and $L$ is the constant factor. NDWI is the third index which have been used to estimate ET and it found suitable to identify water within an image. This index also ranges between +1 to –1, where higher values representing water-logged areas and the lower values associated with vegetation cover [40]. Landsat 8 have band 3 (green) and band 5 (NIR) which are used in the NDWI calculation as indicated in Eq. (3).

$$\mathrm{NDWI} = \frac{\rho_G - \rho_{\mathrm{NIR}}}{\rho_G + \rho_{\mathrm{NIR}}} \tag{8}$$

where ρ is spectral reflectance of Landsat image, $G$ represents band 3 (green) while NIR (near infrared) as band 5. The relationship between vegetation indices and evapotranspiration were analyzed with 9 quarterly images (2018–2019). Regression analysis was performed using Eq. (9) for all the images and indices, by taking numerous random points to understand the relation among ET and vegetation indices in ArcGIS 10.6 software.

$$Y = \alpha + \beta \times X \tag{9}$$

where $Y$ representing dependent variables (NDWI, SAVI, NDVI), β is slope, $X$ is independent variables (evapotranspiration) and α is intercept. The intercept can be removed by set intercept and get relation between two different variables and Pearson's correlation was also computed using Microsoft-Excel 2018.

## 3. Results

### 3.1. Relational study of NDVI and ET

NDVI and ET was calculated as per discussed technique in methodology section and regression analysis was found for all the images. Fig. 3 represents the spatial distribution of NDVI for images of 2019, illustrating the concentration of vegetation in study area. Most of the vegetation cover was found in the central and north-eastern part as per higher NDVI values while surrounding negative values indicating the strong desert climate. The scientists classified NDVI in different categories but most of them indicated two major divisions: vegetation cover with positive values (>0.19) and negative pixels with non-vegetation [41].

The maximum NDVI values were evident throughout the timespan associating lush green vegetation in the selected areas [42]. Detailed maximum and minimum values of all seasons NDVI are presented in Table 2. In every year, values increased during summer while it reduced somehow in winter season [43].

Likewise, the minimum (negative) values got their peak in summer and lowest in winter, which mainly due to strong arid climate (desert) of the region [37]. Also, most of the study area cultivated under high efficiency irrigation system due to which, vegetative proportion (positive values) get approximately constant. However, due to non-availability of water in other parts of study area, reduction of vegetative proportion (high negative value) was resulted, especially in summer when no rainfall occurs [44].

#### 3.1.1. Regression analysis of NDVI and ET

The relationship between NDVI and ET was investigated by regression and correlation of all selected images. Specific trend was observed which varies throughout the year with a maximum value of $R^2$ (0.72) in October-18 and minimum of 0.56 for December-19. In winter season, $R^2$ values remains at 0.61 and 0.57 for both the years, though it got increased to 0.63 and 0.62 in spring respectively. Likewise, to spring season, regression value did not exceed in summer and gone upto 0.62 and 0.60 in both years. However, in autumn regression values gone to 0.72 and 0.67 which was the highest during complete study period (Fig. 4). Overall, the association between both the variables remains consistent up to the mid of the year and then gets enhance in the end. Generally, the relation between NDVI and ET sounds good for the whole period which indicates that this study can be used for approximation purposes.

### 3.2. Relational study of SAVI and ET

The study area mostly consisted of desert, which implies higher reflectance from the soil causing inverse impact on

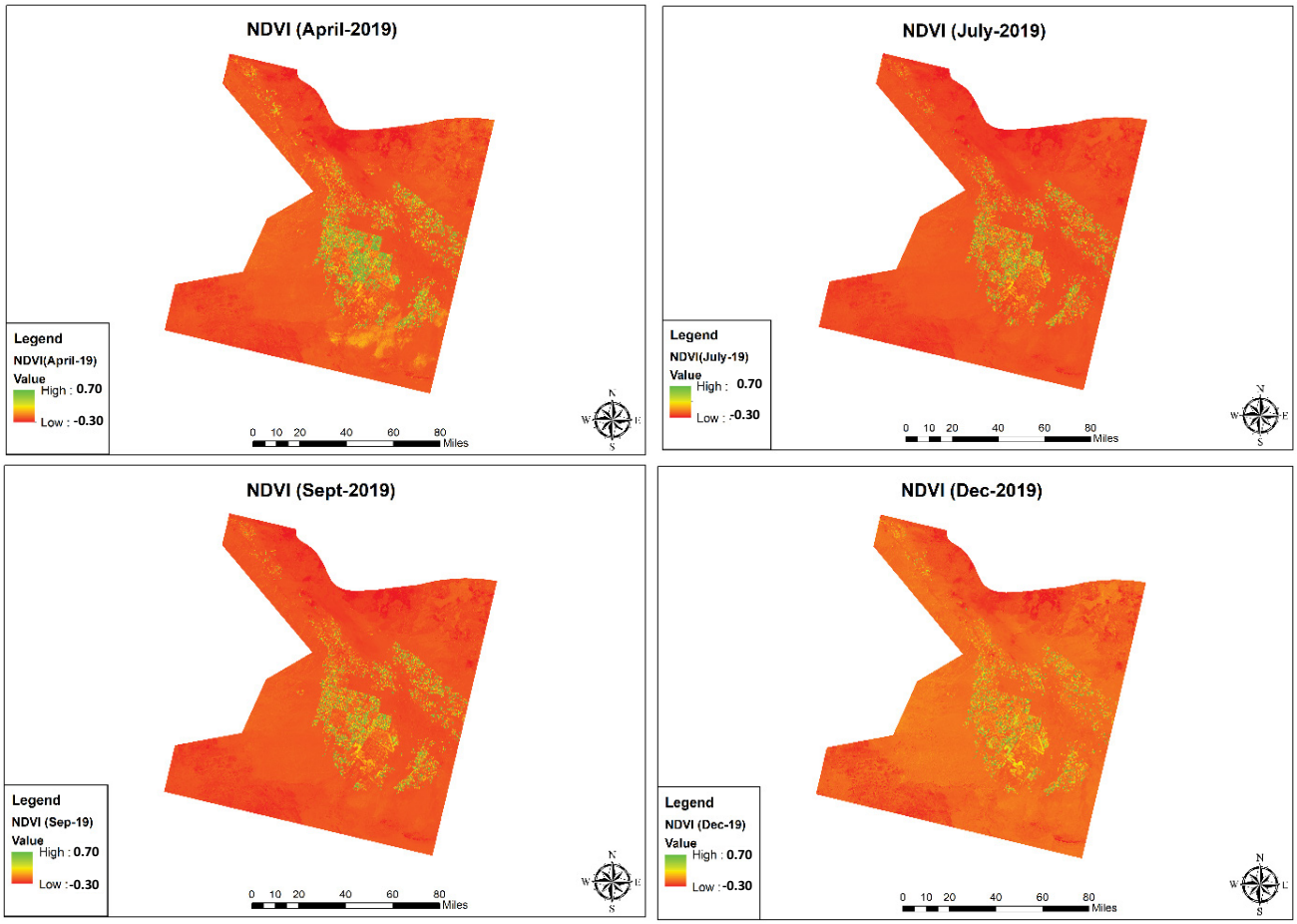


Fig. 3. NDVI map of study area for images of 2019.

Table 2
Maximum and minimum values of NDVI for all images

| Acquisition Date | NDVI values | |
|---|---|---|
| | $NDVI_{min}$ | $NDVI_{max}$ |
| 09-01-18 | –0.12 | 0.52 |
| 14-03-18 | –0.23 | 0.63 |
| 04-07-18 | –0.11 | 0.55 |
| 08-10-18 | –0.036 | 0.57 |
| 11-12-18 | –0.33 | 0.55 |
| 18-04-19 | –0.28 | 0.63 |
| 07-07-19 | –0.046 | 0.67 |
| 09-09-19 | –0.08 | 0.63 |
| 30-12-19 | –0.19 | 0.54 |

reflected digital number (DN) [45]. In order to account for bare soil, correction factor ($L$) was taken as 0.5 as suggested by numerous researchers for different vegetation covers [46]. Graphical representation of SAVI maps indicated higher values in the central and north-eastern part of study area, however some traces was also seen in the north-western side as shown in Fig. 5. The index showed highest values in the month of march and April 2018–2019 while minimum for January-18 respectively.

On average basis, vegetation part presented SAVI index approximately 0.8 indicating healthy vegetation in the area [47]. Meanwhile most pixels other than vegetation area have negative value which depicts the complete bare soil [48].

Detailed values of SAVI and difference between NDVI and SAVI are presented in Table 3. The maximum value difference of NDVI–SAVI showed average value of 0.29 showing stronger influence on DN values, likewise NDVI–SAVI (min) presented much lower difference, exhibiting no effect of SAVI on complete bare soil [49,50].

### *3.2.1. Regression analysis of SAVI and ET*

SAVI index consider the soil reflectance due to which batter values of regression were observed for whole period than NDVI. SAVI remain consistent for most of the images with maximum values of $R^2$ = 0.78 for october-18 and minimum 0.59 in December-2018. In summer and spring season regression behavior was same (~0.65) for both years however for winter it enhanced little to 0.67 (Fig. 6). Collectively, SAVI showed better behaviors with ET than NDVI because of its consistency and higher value for all months (>0.60). Regression analysis of NDVI and

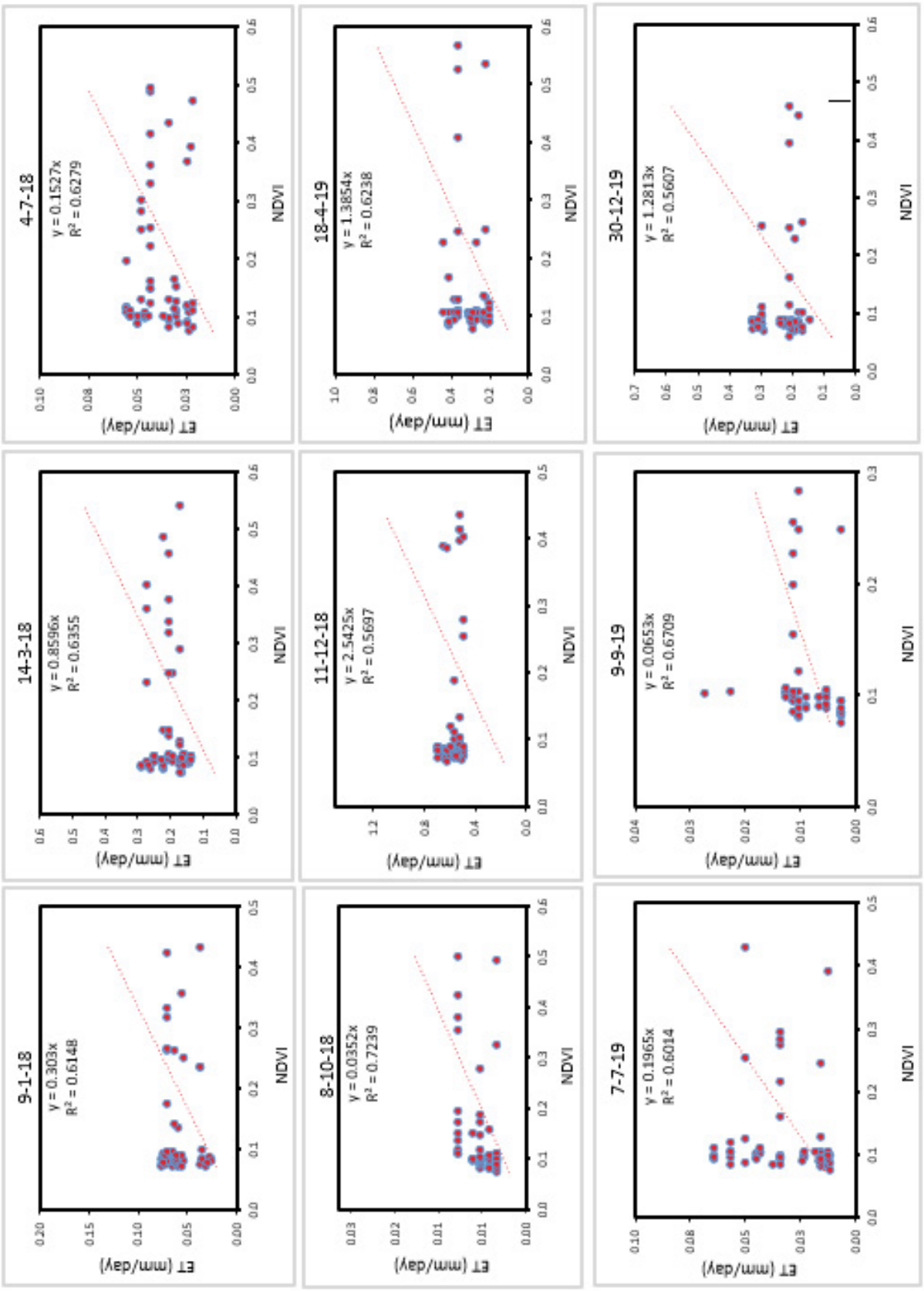


Fig. 4. Regression analysis between NDVI and evapotranspiration (ET) for the whole study period (2018–2019).

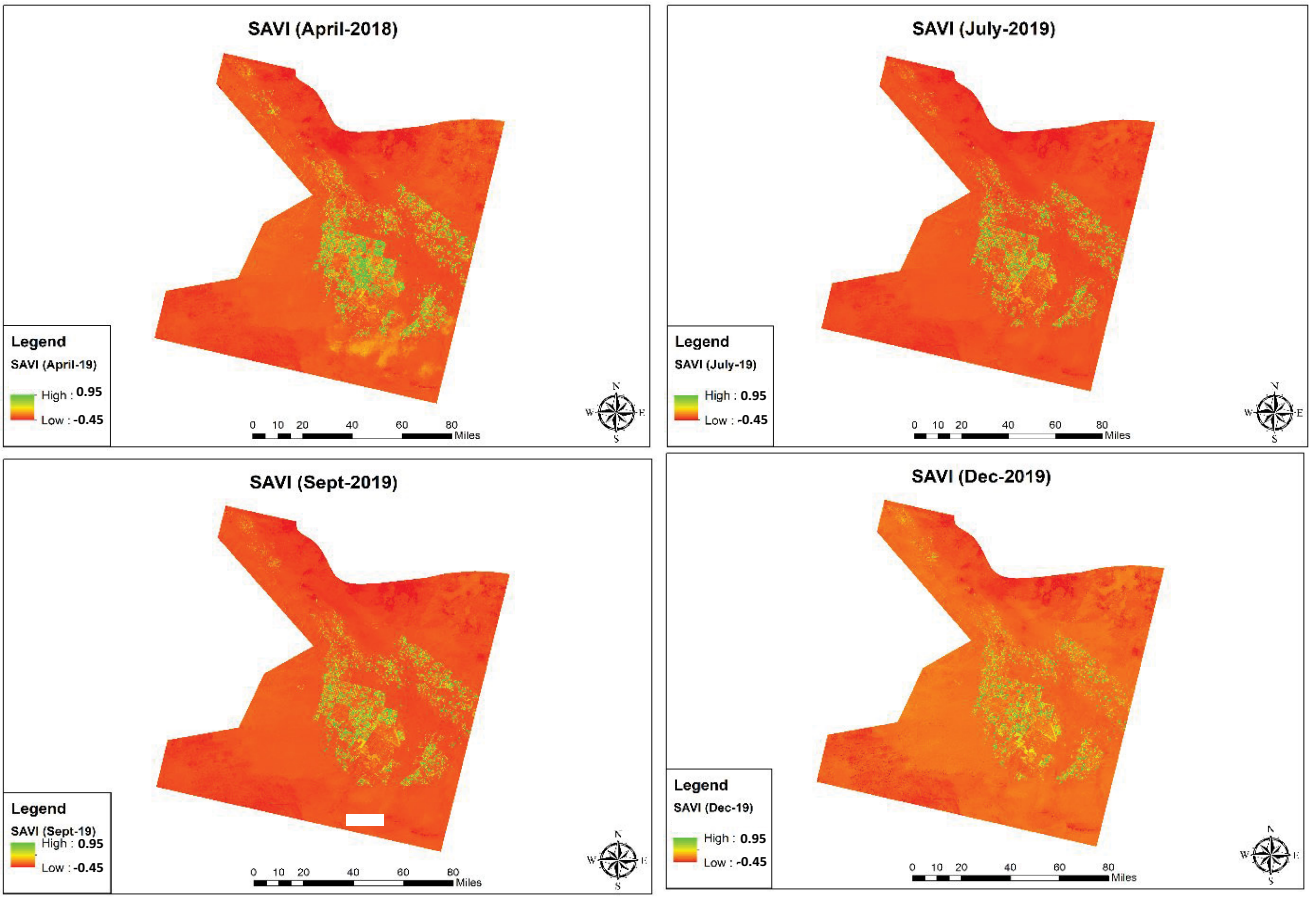


Fig. 5. SAVI map of study area for 2019 images.

Table 3
Maximum and minimum values of SAVI and their difference with NDVI for all images

| Acquisition date | $SAVI_{min}$ | $SAVI_{max}$ | $NDVI–SAVI_{(max)}$ | $NDVI–SAVI_{(min)}$ |
|---|---|---|---|---|
| 09-01-18 | –0.18 | 0.79 | 0.27 | 0.06 |
| 14-03-18 | –0.34 | 0.94 | 0.31 | 0.11 |
| 04-07-18 | –0.17 | 0.83 | 0.28 | 0.06 |
| 08-10-18 | –0.05 | 0.85 | 0.28 | 0.014 |
| 11-12-18 | –0.49 | 0.82 | 0.27 | 0.16 |
| 18-04-19 | –0.42 | 0.98 | 0.35 | 0.14 |
| 07-07-19 | –0.07 | 0.93 | 0.26 | 0.024 |
| 09-09-19 | –0.12 | 0.94 | 0.31 | 0.04 |
| 30-12-19 | –0.28 | 0.81 | 0.27 | 0.09 |
| Average | –0.23 | 0.87 | 0.29 | 0.078 |

SAVI indicated that SAVI has a more positive relationship with evapotranspiration, mostly due to the soil correction factor (0.5) used in its formula [46]. Decent behavior was also due to the fact of healthy crop under Center Pivot Irrigation System which accurately resembles the reflectance from vegetation. Likewise, relation of SAVI was precise just because of same crop, it may vary for mixed landuse-landcover (LULC) [51]. Consequently, the relation of NDVI could be wider in its application because of its non-dependency on same LULC type [37].

### 3.3. Relational study of NDWI and ET

NDWI is known for its considerable relationship with water stress of plant, so it provide a good proxy to plant water deficiency [50]. The detection values for index ranges

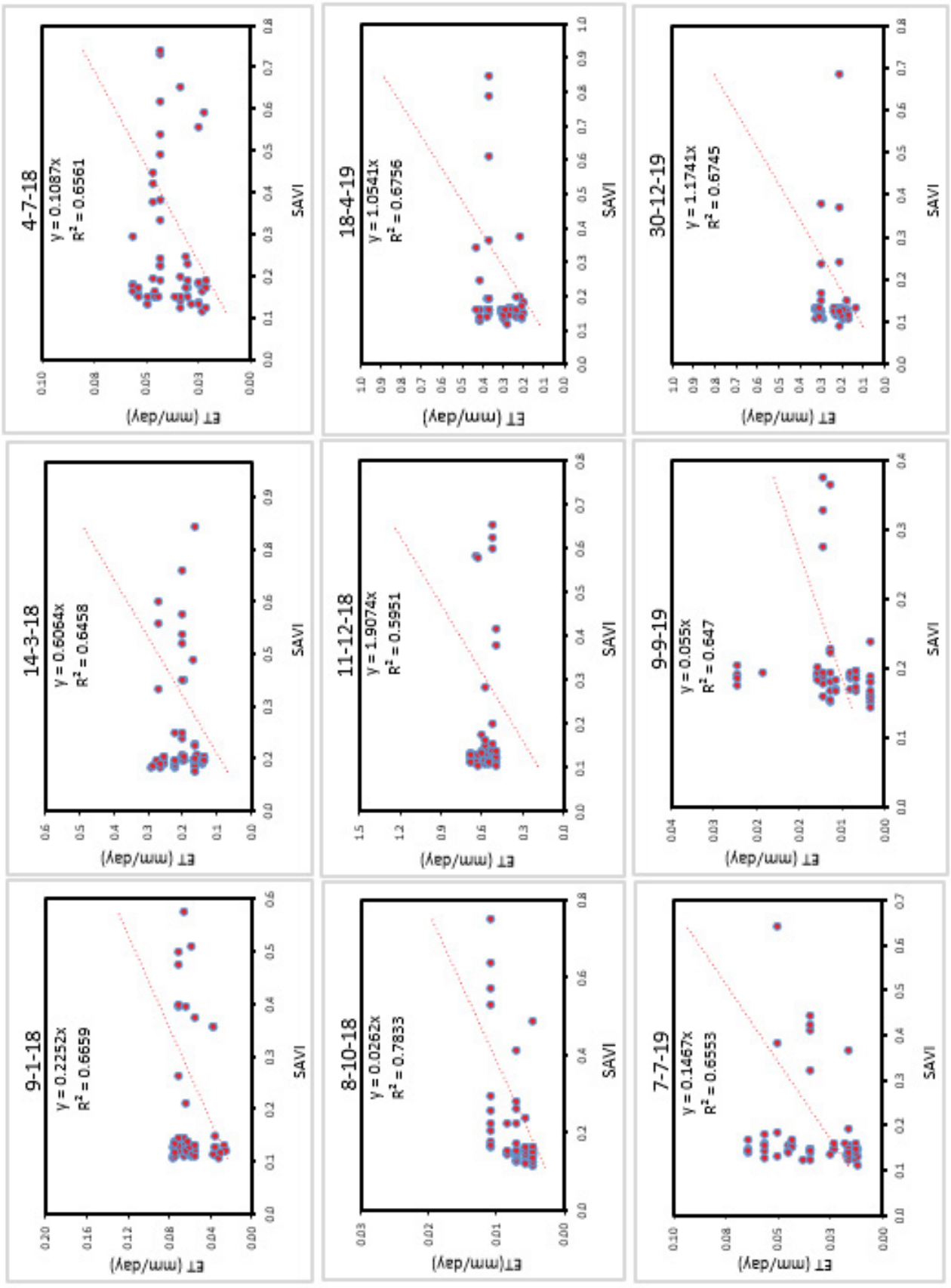


Fig. 6. Regression analysis between SAVI and evapotranspiration (ET) for the whole study period (2018–2019).

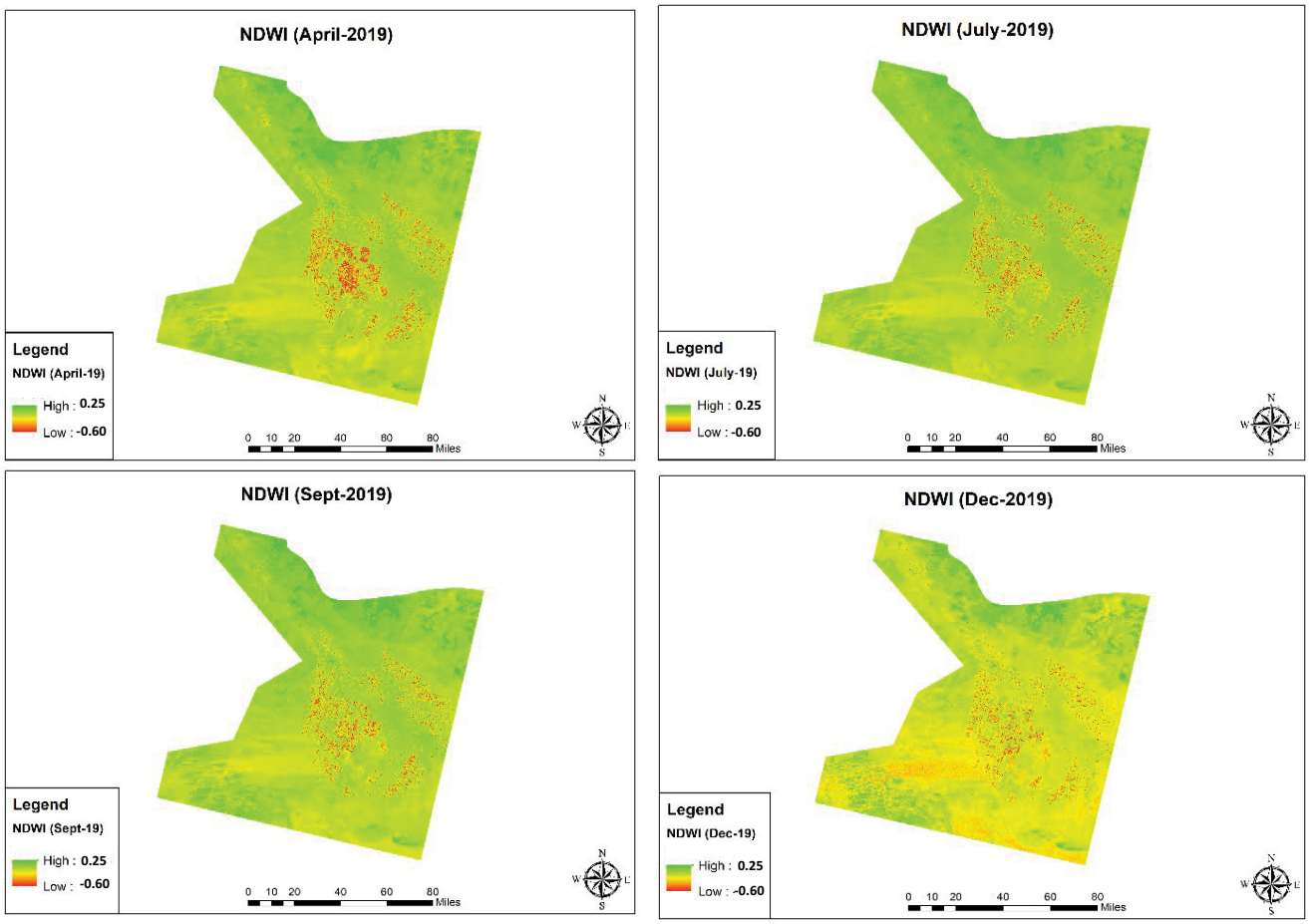


Fig. 7. NDWI map of study area for 2019 images.

between +1 to –1, if NDWI > 0 then it indicates water content, while NDWI ≤ 0 directs the non-water content [52]. In the study area, central parts where vegetation exists showed negative values representing water stress conditions except April which may be due to precipitation events, while surrounding pixels was approximately 0 indicating no water body existence (Fig. 7).

By observing the maximum and minimum values of all months we can access those positive values was lower in the summer season while it enhanced for winter (Table 4). Likewise, negative values were observed on the vegetation cover which remain almost consistent for all seasons indicating that vegetation cover was not under stress and remain same [52].

Table 4
Maximum and minimum values of NDWI for all images

| Acquisition date | NDWI values | |
|---|---|---|
| | $NDWI_{min}$ | $NDWI_{max}$ |
| 09-01-18 | –0.11 | 0.45 |
| 14-03-18 | –0.56 | 0.14 |
| 04-07-18 | –0.51 | 0.04 |
| 08-10-18 | –0.52 | 0.03 |
| 11-12-18 | –0.48 | 0.30 |
| 18-04-19 | –0.57 | 0.22 |
| 07-07-19 | –0.59 | 0.06 |
| 09-09-19 | –0.57 | 0.07 |
| 30-12-19 | –0.48 | 0.19 |

### 3.3.1. Correlation between NDWI and ET

NDWI indicated higher regression values throughout the study period. The spring and autumn of 2018 showed highest regression value (0.90) among whole study period. However, winter and summer season showed slight decrement ($R^2$ = 0.85) but overall good correlation between NDWI and ET.

Likewise in 2019 summer and winter season behave alike (0.85) to preceding year but image from July and September presented some decline to 0.71 and 0.64 respectively (Fig. 8).

Generally, NDWI performs much better for both the years with overall average regression value of 0.85, indicating more promising relation with evapotranspiration than NDVI and SAVI. NDWI is sensitive to stomatal conductance of plant so its use in water content estimation seems more promising, therefore it performs well in dense vegetation of desert climate [53]. NDVI provide evidence of chlorophyll content while NDWI enable to retrieve information of

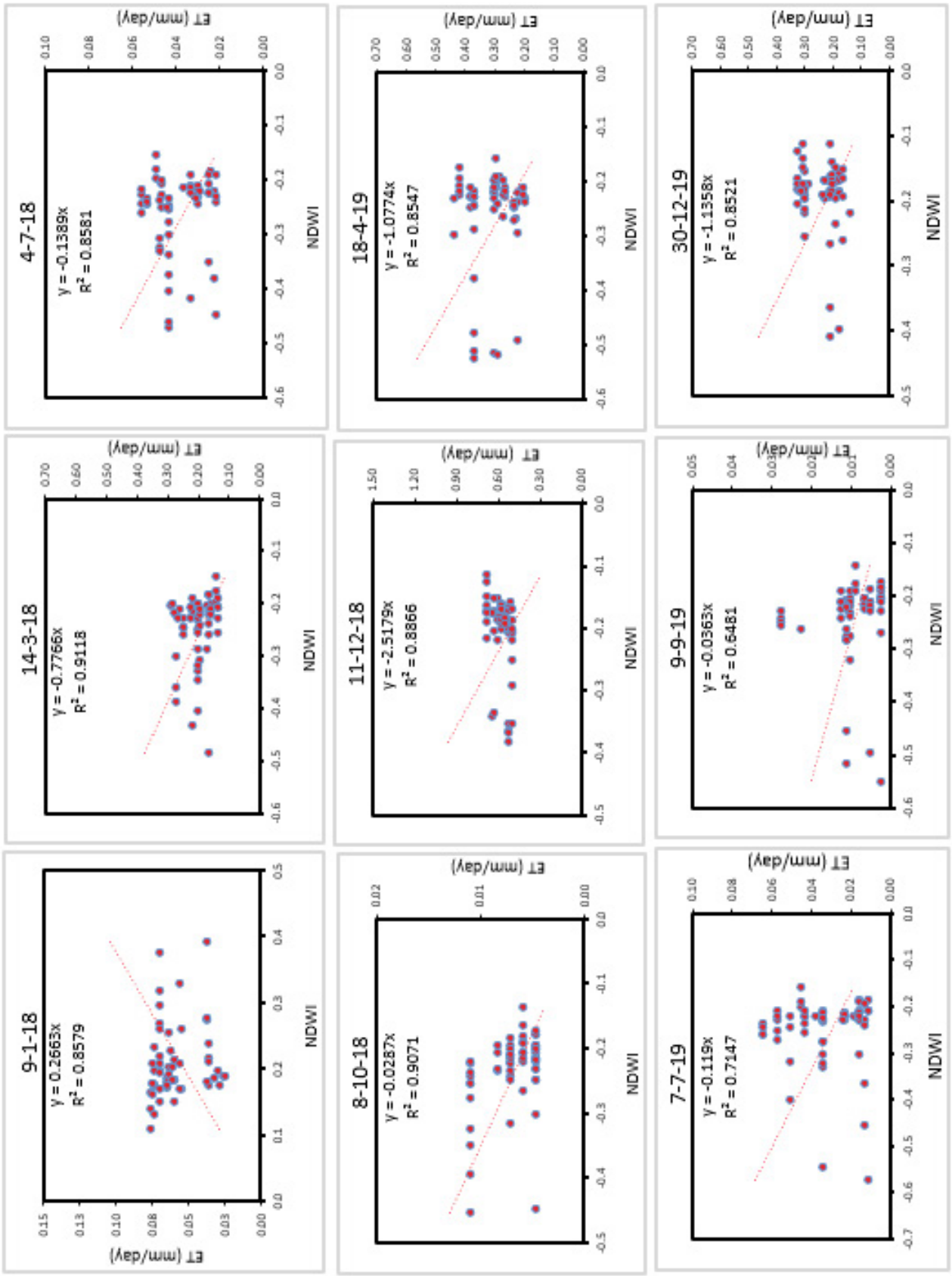


Fig. 8. Regression analysis between NDWI and evapotranspiration (ET) for the whole study period (2018–2019).

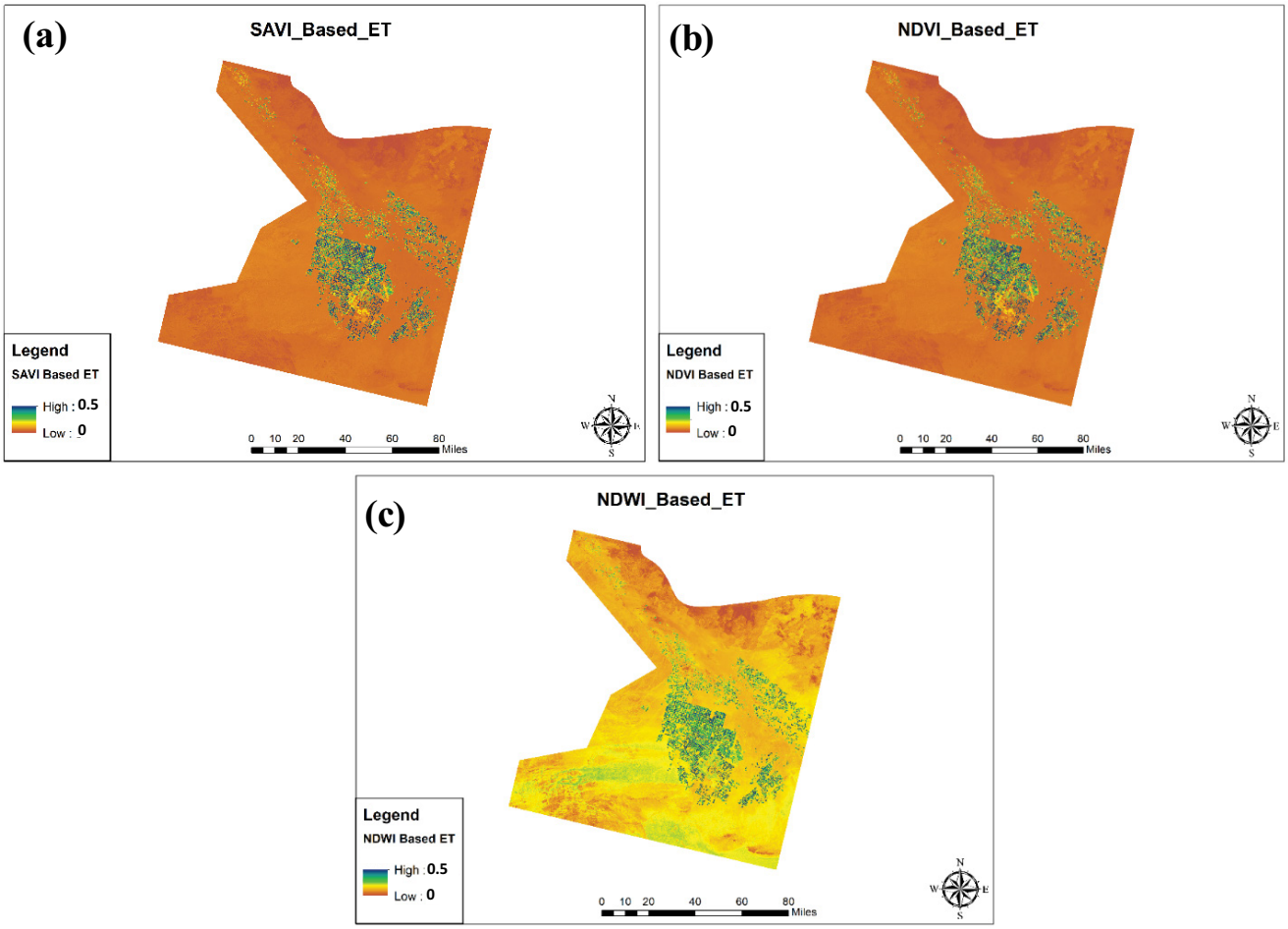


Fig. 9. (a) Map representing evapotranspiration based on NDVI-ET relationship, (b) SAVI-ET relationship and (c) NDWI-ET relationship.

water content within the vegetation therefore it performed well than other indices [54].

Regression model can be applied to estimate fine resolution ET as shown in Fig. 9. Vegetation indices showed promising results due to the homogeneity of the crop, covering nearly 60% area with alfalfa and it may reduce for mixed crops. This approach could be very useful in arid climate where plant transpiration dominates.

## 4. Discussion

Variation in indices is caused by a variety of factors, including meteorological conditions, vegetation proportion, crop kind, soil moisture condition, and vegetation reflectance. The correction factor (0.5) used in SAVI's formula and the fact that most of the study area was covered with alfalfa crop under Center Pivot Irrigation System accurately resembled the spectral response. Regression analysis of NDVI and SAVI revealed that SAVI has a stronger positive relationship with ET. However, this relationship may be precise just for such a certain crop and location, but because it varies, the percentage of accuracy may be thrown off. As a result, because NDVI is not dependent on vegetation cover or kind, its use may be broader. Similarly, canopy conductance is important in the utilization of VI-based ET, which must remain constant [55]. This can only be accomplished by applying consistent water to the crop, which is met in the current study region due to a high-efficiency irrigation system, resulting in a positive relationship. Because of the dominance of plant transpiration and the less wet condition of the soil in arid climates, this strategy could be highly effective. Vegetation indices showed very promising results in this study mainly due to the homogeneity of the crop, which have been covered with alfalfa for more than 60% of the selected area and this precision may reduce for mixed crops due to difference in soil heat flux (Gn). Similar to the VI-ET estimation normally affected by the satellite measurement because of technique by which image acquisition have done, it's been taken for an instance and projected to the whole day, or even part of the day (morning, evening or mid of day). Hence, appropriate understanding must be needed for promising estimation wither direct or by VI's. NDWI known for strong relation with water stress of plant leaves, so it provides good proximity to plant water deficit and normalness. The research region is completely under arid conditions, with only a little limited amount of flora existing within the field. Also, because evaporation

has a very low impact outside of the field area, so the left factor is transpiration, so the NDWI for water content in the leaves dominates more, indicating its ET interdependency for arid climate, which is the main reason why this index leads more in the study. Moreover, NDWI values provide quicker response to the crop water condition than NDVI due to the reason that NDVI has limited capability of water content retrieval information and only provide information of chlorophyll content with no information regarding water quantity within the vegetation.

New satellite sensors with higher spatial and spectral resolution may enhance these relationships and can improve assessment of ET which will assist the farmers about more accurate irrigation management. VI studies for varied crop conditions must be conducted so that long-term evapotranspiration may be calculated on a global scale and used in regional and global models.

## 5. Conclusion

This study mainly focused on the strength of relationship between GLDAS estimated evapotranspiration and Landsat 8 based vegetation indices. As, for the study region three main vegetation indices were selected namely, NDVI, SAVI, and NDWI. Evaluation in this study indicated that NDVI was the least associated with evapotranspiration however, SAVI behaves better throughout the study period. Most promising results were obtained by NDWI which sustains the relationship above 0.85 for most of the images. Hence, it is recommended that for the arid climate like Al-Jawf where dense vegetation was present, the most reliable relationship of vegetation index to estimate ET by Landsat 8 is NDWI. This study provides a better ability to get ET with relational work rather than complex indirect techniques.

As future perspectives, new sensors with higher spatial and spectral resolution (UAV's) may enhance relationships to estimate evapotranspiration indirectly. Similarly, studies based on VI's has to be performed for mixed LULC, so that it can be implemented on a global scale. In further studies reflectance indices, especially lies under thermal infrared band (NIR) of Landsat 8 can provide canopy temperature and may provide good relationship. Moreover, vegetation canopy transpiration index (VCTI) can play vital role in excellent correlation estimation with plant evapotranspiration.

## Conflicts of interest

The authors declare that they have no conflicts of interest.

## References


[1] M. Elhag, A. Psilovikos, I. Manakos, K. Perakis, Application of the SEBS water balance model in estimating daily evapotranspiration and evaporative fraction from remote sensing data over the Nile Delta, Water Resour. Manage., 25 (2011) 2731–2742.

[2] J. Cristóbal, M.C. Anderson, Validation of a Meteosat Second Generation solar radiation dataset over the northeastern Iberian Peninsula, Hydrol. Earth Syst. Sci., 17 (2013) 163–175.

[3] M. Mohammadian, R. Arfania, H. Sahour, Evaluation of SEBS algorithm for estimation of daily evapotranspiration using landsat-8 dataset in a Semi-Arid Region of Central Iran, Open J. Geol., 7 (2017) 335–347.

[4] N. Ghilain, A. Arboleda, F. Gellens-Meulenberghs, Evapotranspiration modelling at large scale using near-real time MSG SEVIRI derived data, Hydrol. Earth Syst. Sci., 15 (2011) 771–786.

[5] S.Z. Losgedaragh, M. Rahimzadegan, Evaluation of SEBS, SEBAL, and METRIC models in estimation of the evaporation from the freshwater lakes (Case study: Amirkabir dam, Iran), J. Hydrol., 561 (2018) 523–531.

[6] M. Awais, W. Li, M.J.M. Cheema, Q.U. Zaman, A. Shaheen, B. Aslam, W. Zhu, M. Ajmal, M. Faheem, S. Hussain, A.A. Nadeem, M.M. Afzal, C. Liu, UAV-based remote sensing in plant stress imagine using high-resolution thermal sensor for digital agriculture practices: a meta-review, Int. J. Environ. Sci. Technol., (2022) 1–18, doi: 10.1007/s13762-021-03801-5.

[7] M. Awais, W. Li, M. Cheema, S. Hussain, A. Shaheen, B. Aslam, C. Liu, A. Ali, Assessment of optimal flying height and timing using high-resolution unmanned aerial vehicle images in precision agriculture, Int. J. Environ. Sci. Technol., (2021) 1–18.

[8] M. Rodell, P. Houser, U. Jambor, J. Gottschalck, K. Mitchell, C.-J. Meng, K. Arsenault, B. Cosgrove, J. Radakovich, M. Bosilovich, The Global Land Data Assimilation System, Bull. Am. Meteorol., 85 (2004) 381–394.

[9] J.P. Moiwo, F. Tao, W. Lu, Analysis of satellite-based and in situ hydro-climatic data depicts water storage depletion in North China Region, Hydrol. Processes, 27 (2013) 1011–1020.

[10] E. Forootan, R. Rietbroek, J. Kusche, M.A. Sharifi, J.L. Awange, M. Schmidt, P. Omondi, J. Famiglietti, Separation of large scale water storage patterns over Iran using GRACE, altimetry and hydrological data, Remote Sens. Environ., 140 (2014) 580–595.

[11] A. Elbeltagi, N. Kumari, J.K. Dharpure, A. Mokhtar, K. Alsafadi, M. Kumar, B. Mehdinejadiani, H. Ramezani Etedali, Y. Brouziyne, T.J.W. Islam, Prediction of combined terrestrial evapotranspiration index (CTEI) over large river basin based on machine learning approaches, Water, 13 (2021) 547, doi: 10.3390/w13040547.

[12] J. Won, J. Seo, J. Lee, O. Lee, S. Kim, Vegetation drought vulnerability mapping using a copula model of vegetation index and meteorological drought index, Remote Sens. Environ., 13 (2021) 5103, doi: 10.3390/rs13245103.

[13] E.P. Glenn, P.L. Nagler, A.R. Huete, Vegetation index methods for estimating evapotranspiration by remote sensing, Surv. Geophys., 31 (2010) 531–555.

[14] E. Bari, N.J. Nipa, B. Roy, Association of vegetation indices with atmospheric & biological factors using MODIS time series products, Environ. Challenges, 5 (2021) 100376, doi: 10.1016/j.envc.2021.100376.

[15] F. Hall, P. Sellers, First international satellite land surface climatology project (ISLSCP) field experiment (FIFE) in 1995, J. Geophys. Res.: Atmos., 100 (1995) 25383–25395.

[16] M. Chiesi, B. Rapi, P. Battista, L. Fibbi, B. Gozzini, R. Magno, A. Raschi, F. Maselli, Combination of ground and satellite data for the operational estimation of daily evapotranspiration, Eur. J. Remote Sens., 46 (2013) 675–688.

[17] Y. Zhang, S. Yang, W. Ouyang, H. Zeng, M. Cai, Applying multi-source remote sensing data on estimating ecological water requirement of grassland in ungauged region, Procedia Environ. Sci., 2 (2010) 953–963.

[18] H. Wang, Z. Li, L. Cao, R. Feng, Y. Pan, Response of NDVI of natural vegetation to climate changes and drought in China, Land, 10 (2021) 966, doi: 10.3390/land10090966.

[19] C. Domenikiotis, M. Spiliotopoulos, E. Tsiros, N. Dalezios, Early cotton production assessment in Greece based on a combination of the drought Vegetation Condition Index (VCI) and the Bhalme and Mooley Drought Index (BMDI), Int. J. Remote Sens., 25 (2004) 5373–5388.

[20] J. Park, J. Baik, M. Choi, Satellite-based crop coefficient and evapotranspiration using surface soil moisture and vegetation indices in Northeast Asia, Catena, 156 (2017) 305–314.

[21] M. Awais, W. Li, S. Hussain, M.J.M. Cheema, W. Li, R. Song, C. Liu, Comparative evaluation of land surface temperature images from unmanned aerial vehicle and satellite observation for agricultural areas using in situ data, Agriculture, 12 (2022) 184, doi: 10.3390/agriculture12020184.

[22] M. Spiliotopoulos, A. Loukas, Hybrid methodology for the estimation of crop coefficients based on satellite imagery and ground-based measurements, Water, 11 (2019) 1364, doi: 10.3390/w11071364.
[23] J.A. Sobrino, N. Souza da Rocha, D. Skoković, P. Suélen Käfer, R. López-Urrea, J.C. Jiménez-Muñoz, S.B. Alves Rolim, Evapotranspiration estimation with the S-SEBI method from Landsat 8 data against Lysimeter measurements at the Barrax site, Spain, Remote Sens., 13 (2021) 3686, doi: 10.3390/rs13183686.
[24] L. Caturegli, S. Matteoli, M. Gaetani, N. Grossi, S. Magni, A. Minelli, G. Corsini, D. Remorini, M. Volterrani, Effects of water stress on spectral reflectance of bermudagrass, Sci. Rep., 10 (2020) 1–12.
[25] N. Jovanovic, C.L. Garcia, R.D. Bugan, I. Teich, C.M.G. Rodriguez, Validation of remotely-sensed evapotranspiration and NDWI using ground measurements at Riverlands, South Africa, Water S.A., 40 (2014) 211–220.
[26] B. Almutairi, A. El Battay, M.A. Belaid, N.A.H. Musa, Comparative study of SAVI and NDVI vegetation indices in Sulaibiya Area (Kuwait) using worldview satellite imagery, Int. J. Geosci. Geomat., 1 (2013) 50–53.
[27] D.P. Groeneveld, W.M. Baugh, Correcting satellite data to detect vegetation signal for eco-hydrologic analyses, J. Hydrol., 344 (2007) 135–145.
[28] S.H. Mahmoud, Delineation of potential sites for groundwater recharge using a GIS-based decision support system, Environ. Earth Sci., 72 (2014) 3429–3442.
[29] S. Chowdhury, M. Al-Zahrani, Characterizing water resources and trends of sector wise water consumptions in Saudi Arabia, J. King Saud Univ. Eng. Sci., 27 (2015) 68–82.
[30] S. Chowdhury, M. Al-Zahrani, A. Abbas, Implications of climate change on crop water requirements in arid region: an example of Al-Jouf, Saudi Arabia, J. King Saud Univ. Eng. Sci., 28 (2016) 21–31.
[31] O.M. Lopez Valencia, K. Johansen, B.J.L. Aragon Solorio, T. Li, R. Houborg, Y. Malbeteau, S. Almashharawi, M. Altaf, E.M. Fallatah, H.P. Dasari, Mapping groundwater abstractions from irrigated agriculture: big data, inverse modeling and a satellite-model fusion approach, Hydrol. Earth Syst. Sci., 24 (2020) 5251–5277.
[32] M.H. Jahangir, M. Arast, Estimation of surface soil moisture based on improved multi-index models and surface energy balance system, Nat. Resour. Res., 30 (2021) 789–804.
[33] A. Nagy, A. Szabó, O.D. Adeniyi, J. Tamás, Wheat yield forecasting for the Tisza River catchment using Landsat 8 NDVI and SAVI time series and reported crop statistics, Agronomy, 11 (2021) 652, doi: 10.3390/agronomy11040652.
[34] J.M. Norman, M.C. Anderson, W.P. Kustas, A.N. French, J. Mecikalski, R. Torn, G.R. Diak, T. Schmugge, B.C.W. Tanner, Remote sensing of surface energy fluxes at $10^1$-m pixel resolutions, Water Resour. Res., 39 (2003), doi: 10.1029/2002WR001775.
[35] F. Firouzi, T. Tavosi, P. Mahmoudi, Investigating the sensitivity of NDVI and EVI vegetation indices to dry and wet years in arid and semi-arid regions (Case study: Sistan plain, Iran), Sci. Res. Quart. Geogr. Data, 28 (2019) 163–179.
[36] M.T. Schnur, H. Xie, X. Wang, Estimating root zone soil moisture at distant sites using MODIS NDVI and EVI in a semi-arid region of southwestern USA, Ecol. Inform., 5 (2010) 400–409.
[37] J. Wang, J.-f. Huang, X.-z. Wang, M.-t. Jin, Z. Zhou, Q.-y. Guo, Z.-w. Zhao, W.-j. Huang, Y. Zhang, X.-d. Song, Estimation of rice phenology date using integrated HJ-1 CCD and Landsat-8 OLI vegetation indices time-series images, J. Zhejiang Univ. Sci. B, 16 (2015) 832–844.
[38] V. Chowdary, R.V. Chandran, N. Neeti, R. Bothale, Y. Srivastava, P. Ingle, D. Ramakrishnan, D. Dutta, A. Jeyaram, J. Sharma, Assessment of surface and sub-surface waterlogged areas in irrigation command areas of Bihar state using remote sensing and GIS, Agric. Water Manage., 95 (2008) 754–766.
[39] H. Hashim, Z. Abd Latif, N.A. Adnan, Urban Vegetation Classification with NDVI Thresold Value Method with Very High Resolution (VHR) Pleiades Imagery, The International Archives of the Photogrammetry, Remote Sensing and Spatial Information Sciences, Volume XLII-4/W16, 6th International Conference on Geomatics and Geospatial Technology (GGT 2019), 1–3 October 2019, Kuala Lumpur, Malaysia, 2019, pp. 237–240.
[40] Y. Julien, J.A. Sobrino, Introducing the time series change visualization and interpretation (TSCVI) method for the interpretation of global NDVI changes, Int. J. Appl. Earth Obs., 96 (2021) 102268, doi: 10.1016/j.jag.2020.102268.
[41] S.S. Naif, D.A. Mahmood, M.H. Al-Jiboori, Seasonal normalized difference vegetation index responses to air temperature and precipitation in Baghdad, Open Agric., 5 (2020) 631–637.
[42] J. Mallick, M.K. AlMesfer, V.P. Singh, I.I. Falqi, C.K. Singh, M. Alsubih, N.B. Kahla, Evaluating the NDVI–rainfall relationship in Bisha Watershed, Saudi Arabia using non-stationary modeling technique, Atmosphere, 12 (2021) 593, doi: 10.3390/atmos12050593.
[43] N.R. Wilson, L.M. Norman, M. Villarreal, L. Gass, R. Tiller, A. Salywon, Comparison of remote sensing indices for monitoring of desert cienegas, Arid. Land Res. Manage., 30 (2016) 460–478.
[44] V. Vani, V.R. Mandla, Comparative Study of NDVI and SAVI vegetation indices in Anantapur district semi-arid areas, Int. J. Civ. Eng. Technol., 8 (2017) 559–566.
[45] Z. Zhen, S. Chen, T. Yin, E. Chavanon, N. Lauret, J. Guilleux, M. Henke, W. Qin, L. Cao, J. Li, Using the negative soil adjustment factor of soil adjusted vegetation index (SAVI) to resist saturation effects and estimate leaf area index (LAI) in dense vegetation areas, Sensors, 21 (2021) 2115, doi: 10.3390/s21062115.
[46] H. Ren, G. Zhou, F. Zhang, Using negative soil adjustment factor in soil-adjusted vegetation index (SAVI) for aboveground living biomass estimation in arid grasslands, Remote Sens. Environ., 209 (2018) 439–445.
[47] C. Polykretis, M.G. Grillakis, D.D. Alexakis, Exploring the impact of various spectral indices on land cover change detection using change vector analysis: a case study of Crete Island, Greece, Remote Sens. Environ., 12 (2020) 319, doi: 10.3390/rs12020319.
[48] K. Katarzyna, S. Justyna, S. Jakub, S. Marcin, Estimation of bare soil moisture from remote sensing indices in the 0.4–2.5 mm spectral range, Trans. Aerosp. Res., 2021 (2021) 1–11.
[49] V.S. da Silva, G. Salami, M.I.O. da Silva, E.A. Silva, J.J. Monteiro Junior, E. Alba, Methodological evaluation of vegetation indexes in land use and land cover (LULC) classification, Geol. Ecol. Landscapes, 4 (2020) 159–169.
[50] L. Ji, L. Zhang, B. Wylie, Analysis of dynamic thresholds for the normalized difference water index, Photogramm. Eng. Remote Sens., 75 (2009) 1307–1317.
[51] X. Wu, Y. Xu, J. Shi, Q. Zuo, T. Zhang, L. Wang, X. Xue, A.J.A. Ben-Gal, F. Meteorology, Estimating stomatal conductance and evapotranspiration of winter wheat using a soil-plant water relations-based stress index, Agric. For. Meteorol., 303 (2021) 108393, doi: 10.1016/j.agrformet.2021.108393.
[52] D. Marusig, F. Petruzzellis, M. Tomasella, R. Napolitano, A. Altobelli, A. Nardini, Correlation of field-measured and remotely sensed plant water status as a tool to monitor the risk of drought-induced forest decline, Forests, 11 (2020) 77, doi: 10.3390/f11010077.
[53] M. Awais, W. Li, M.J.M. Cheema, S. Hussain, T.S. AlGarni, C. Liu, A. Ali, Remotely sensed identification of canopy characteristics using UAV-based imagery under unstable environmental conditions, Environ. Technol. Innovation, 22 (2021) 101465, doi: 10.1016/j.eti.2021.101465.
[54] M. Elhag, Understanding of photosynthetically active radiation index under soil salinity variation using remote sensing practices in arid environments, Desal. Water Treat., 112 (2018) 171–178.
[55] M. Elhag, J. Bahrawi, S. Boteva, Input/output inconsistencies of daily evapotranspiration conducted empirically using remote sensing data in arid environments, Open Geosci., 13 (2021) 321–334.